



Exploring adsorbent potential: Investigating the characteristics of macadamia husk char from pilot-scale gasification

Vu Ngoc Linh¹, Thi Mai Thanh Dinh², Thu Phuong Nguyen³, Phuong Thu Le², Thi Hai Do⁴, Trung Dung Nguyen⁵, Hong Nam Nguyen^{2,*}

¹ Faculty of Engineering Physics and Nanotechnology, University of Engineering and Technology, Vietnam National University, 144 Xuan Thuy, Dich Vong Hau, Cau Giay, Hanoi 100000, VIETNAM

² University of Science and Technology of Hanoi, Vietnam Academy of Science and Technology, 18 Hoang Quoc Viet, Cau Giay, Hanoi 100000, VIETNAM

³ Institute for Tropical Technology, Vietnam Academy of Science and Technology, 18 Hoang Quoc Viet, Cau Giay, Hanoi 100000, VIETNAM

⁴ Faculty of Basic Science, Hanoi University of Mining and Geology, 18 Pho Vien, Duc Thang, Nam Tu Liem, Hanoi 100000, VIETNAM

⁵ Faculty of Physical and Chemical Engineering, Le Quy Don Technical University, 236 Hoang Quoc Viet, Bac Tu Liem, Hanoi 100000, VIETNAM

* Email: nguyen-hong.nam@usth.edu.vn

ARTICLE INFO

Received: 29/03/2024

Accepted: 21/05/2024

Published: 30/12/2024

Keywords:

macadamia residues;
 gasification; pilot scale;
 CO₂ adsorbent

ABSTRACT

Establishing a comprehensive database of char properties from pilot-scale gasification is crucial for identifying optimal applications for carbonaceous residues and advancing the sustainability of this technology. This study explores the intricate characteristics of macadamia husk char generated through pilot-scale gasification, highlighting its potential utility. The resulting char exhibits a porous structure primarily composed of micropores, with a heterogeneous distribution of inorganic minerals, notably K (12 mg g⁻¹) and Ca (41 mg g⁻¹), enhancing adsorption capabilities. Additionally, the surface is rich in oxygen-containing functional groups, such as carbonyl, carboxyl, and hydroxyl moieties, enhancing CO₂ adsorption. The results emphasize the practicality of using macadamia husk for large-scale gasification, which can produce solid adsorbents. This dataset makes a substantial contribution to enhancing the sustainability of biomass gasification.

Introduction

The macadamia nut is among the most sought-after food in the world due to its wide array of health benefits. Global macadamia nut production has steadily increased over the past decade, reaching an estimated 78,415 tons in 2022 [1]. Forecasts suggest a constant rise in global demand for macadamia products, leading to the expansion of production.

The primary product of the macadamia nut is its kernel, comprising roughly 30 % of the nut's weight, while the remainder consists of husk (MH) and nutshell (MNS) [2]. This results in an estimated annual production of nearly 183 million tons of macadamia residues. Currently, macadamia residues are underutilized, primarily discarded or incinerated, with only a small fraction repurposed on-site for inefficient applications such as soil fertilization and poultry feed. This

inefficient management raises concerns about environmental and health impacts and resource wastage. Hence, there is a pressing need for research to explore high-value applications for macadamia residues, contributing to sustainable farming practices. Previous studies have suggested that macadamia residues, due to their wood-like characteristics, hold great promise as biomass fuel for energy conversion technologies such as gasification [3,4].

Gasification is the thermochemical process of converting carbon-containing materials into gases through partial oxidation reactions at high temperatures, typically between 700 °C to 1400 °C [5]. This process involves the reaction of carbon with air, oxygen, steam, carbon dioxide, or a mixture of these gases. The resulting product, known as syngas, primarily consists of CO and H₂, alongside N₂, CO₂, and CH₄. Syngas can be utilized directly in combustion chambers or gas engines to generate heat, power, or electricity for various applications. It also holds potential as a feedstock for synthesizing methane, hydrogen, biofuels, and chemicals, although these applications are still in the experimental stage [6].

MNS has garnered significant research attention globally due to its physicochemical properties akin to wood, making it suitable for various applications, notably the synthesis of carbonaceous materials like activated carbon and graphene-like carbon. However, MH has received less focus, with limited applications. Thus, utilizing MH in biomass gasification processes is crucial, offering a sustainable solution for managing its abundant waste volume. Hence, MH was chosen as the operating material for the pilot-scale gasification system.

Emitting greenhouse gases such as CO₂, CH₄, and N₂O into the atmosphere is a serious issue as it can lead to climate change. CO₂ is of particular concern among greenhouse gases as it is the primary driver of global warming [7]. This results in significant environmental impacts on land, causing severe droughts, altering rainfall patterns, exacerbating heatwaves, melting ice caps, and rising sea levels [8].

To mitigate CO₂ emissions into the atmosphere, many studies aim to develop new and advanced methods for efficient CO₂ capture. In the CO₂ capture industry, CO₂ is absorbed in amine-based solutions [9]. However, this method has drawbacks such as high equipment corrosion risk, additional energy required for solvent regeneration, and the generation of waste sludge. Solid material-based adsorption methods are easier to handle and not prone to corrosion. Recent studies on biochar CO₂ adsorption have shown that biochar from

agricultural residues can effectively capture CO₂ and can be scaled up [10,11].

Previous laboratory-scale studies have indicated the potential of residual char from MH gasification as a viable CO₂ adsorbent. However, significant variations in conversion conditions, such as temperature and reactant composition, can lead to qualitative and quantitative differences in the characteristics of the two types of MH gasification char. These disparities may directly influence the feasibility of utilizing MH gasification char as an adsorbent material in practical large-scale systems. Therefore, to accurately assess the feasibility and viability of employing MH as a biomass feedstock for simultaneous energy and adsorbent material production, it is imperative to investigate the CO₂ adsorption capacity of MH gasification char at pilot scale under conditions closely resembling real-world scenarios.

Experimental

Gasification of macadamia husk

The experimental gasification system utilized in this study is a type of fixed-bed downdraft gasifier, specifically PP20 20kW model, abbreviated as PP20, manufactured by All Power Labs. The system comprises three main components: the gasifier unit, the filtration unit, and the internal combustion engine, as depicted in Fig 1 below.



Fig. 1: The commercial downdraft fixed-bed gasifier (PP20 All Power Lab)

Primarily, 100 kg of raw MH is introduced into the system via a designated hopper. Once the system is activated, the biomass progresses through distinct stages including drying, pyrolysis, and gasification. Following this, the resultant syngas is purified through a cyclone to eliminate impurities, before being employed as fuel in a gas engine coupled with a generator to generate electricity.

After the gasification process of MH using the PP20 system concludes, the residual chars are collected from the char container situated adjacent to the reactor chamber. In reality, the ratio of the recovered char mass from the char container to the input MH mass was found to be approximately 27.1 %, which equivalent to a char yield of 27.1 kg per 100 kg of raw MH.

Characterization of gasified chars

Functional group analysis on the surface of the chars was conducted using a PerkinElmer UATR-FTIR spectrometer. This spectrometer has a mid-infrared range of 500 to 4000 cm^{-1} and a resolution of 4 cm^{-1} . A Jeol JSX - 1000S X-ray fluorescence spectrometer (XRF) was used to determine the elemental composition of the created chars. The Micromeritics ASAP 2060 was used to evaluate the adsorption/desorption characteristics of N_2 in MH char. After a 6-hour period of outgassing at a temperature of 300 $^{\circ}\text{C}$, the char sample underwent examination. The data pertaining to adsorption and desorption ranged from 0 to 0.99 relative pressure (p/p_0). The Brunauer-Emmett-Teller (BET), Barrett-Joyner-Halenda (BJH), and t-plot techniques were used to quantitatively determine the surface areas of total, micropore, and mesopore regions, as well as the pore volume of MH chars.

CO_2 adsorption

The CO_2 gas adsorption experiment was conducted on the Macro Thermogravimetric Analyzer (Macro-TGA) system. Each type of gas was controlled by a separate flowmeter. The biomass sample was placed in a container tray attached to the lifting column, and the sample mass was continuously measured by a balance and recorded by a computer every 5 seconds. The flow rate of CO_2 gas was set to 5 L min^{-1} , and the amount of MH gasified char used for the experiment was 0.3 grams. N_2 gas was used in the desorption process, with a flow rate equal to that of the CO_2 gas. The CO_2 gas adsorption process was tested at atmospheric pressure and room temperature of 25 $^{\circ}\text{C}$.

Results and discussion

Functional group composition on char surface

The surface functional group arrangement of MH gasified char from the PP20 system is illustrated in Fig. 2. Generally, the composition of surface functional groups at the pilot scale closely resembles that of laboratory-scale chars. However, char produced

through the PP20 system exhibits notably higher intensity in FTIR spectra compared to laboratory-scale processes [3]. This suggests a greater abundance of functional groups linked to molecular bonds on the char surface at the pilot scale, along with peak position displacements indicating variations in hybridization or electron distribution within molecular bonds between the two char types.

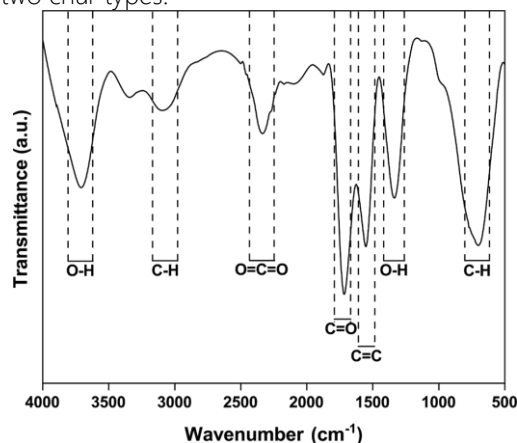


Fig. 2: FTIR spectra of MH gasified char

FTIR spectrum analysis identified bending C-H bonds (at 700 cm^{-1}), O-H bonds (at 1340 cm^{-1}), C=C bonds (at 1544 cm^{-1}), and C=O bonds (at 1714 cm^{-1}) on the surface of MH gasified char from the PP20 system. The intensity of peaks in the range of 2000 to 4000 cm^{-1} was significantly higher compared to laboratory-scale char, particularly peaks corresponding to O=C=O, C-H, and O-H bonds (at 2337 cm^{-1} , 3100 cm^{-1} , and 3740 cm^{-1} , respectively). This difference is likely due to the higher operational temperature (> 1000 $^{\circ}\text{C}$) of the PP20 system compared to laboratory-scale gasification (950 $^{\circ}\text{C}$) [3].

The abundance of surface functional groups, including carbonyl, carboxyl, and hydroxyl, may enhance its CO_2 adsorption capacity. This study underscores the CO_2 adsorption potential of MH char under standard gasification conditions [12,13].

Structural properties of char

The isothermal nitrogen adsorption-desorption curves and distribution of pore width of the gasified char obtained from macadamia husks collected from the PP20 system are illustrated in Fig 3a and 3b. In addition, the Table 1 provides comprehensive data on the specific surface area, micro-meso pore surface area, and pore volume, obtained through the BET, t-plot, and BJH methods. The findings indicate that the gasified char derived from MH in the PP20 system demonstrates a total surface area of $S_{\text{BET}} = 37.8 \text{ m}^2 \text{ g}^{-1}$.

This result is similar to the gasified char generated at elevated temperatures using air as a reactant for different agricultural biomass sources, including rice husk ($S_{\text{BET}} = 32.3 \text{ m}^2 \text{ g}^{-1}$) [14], corn stover ($S_{\text{BET}} = 23.9 \text{ m}^2 \text{ g}^{-1}$) [15], and wood biomass, specifically pine sawdust ($S_{\text{BET}} = 52 \text{ m}^2 \text{ g}^{-1}$) [16]. Furthermore, the gasified char derived from MH in the PP20 system exhibits a predominantly porous structure characterized by micro-sized pores (width $\geq 2 \text{ nm}$). These pores possess a surface area (S_{Micro}) of $14 \text{ m}^2 \text{ g}^{-1}$ and a volume (V_{Micro}) of $0.0077 \text{ cm}^3 \text{ g}^{-1}$. The identification of micro-sized pores suggests that the gasified char derived from macadamia shell residues holds promise as a viable adsorbent material for pollutants with small molecular diameters, such as CO_2 , on an experimental scale.

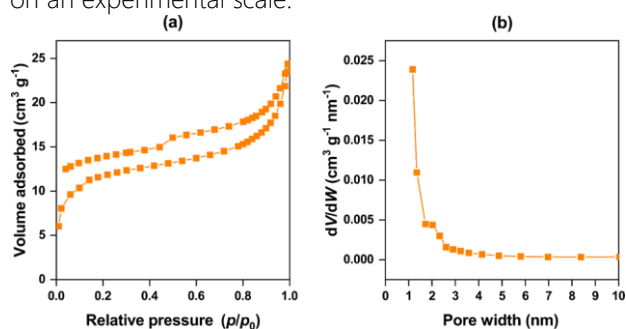


Fig. 3: (a) N_2 adsorption/desorption isotherms and (b) distribution of pore width

Moreover, the analysis of the structural characteristics shows that the porosity of the gasified char produced from MH on the PP20 system experiences a notable decrease compared to the gasified char formed in a controlled laboratory setting, which was found to have an S_{BET} value of $399 \text{ m}^2 \text{ g}^{-1}$ and a V_{BET} value of $0.236 \text{ cm}^3 \text{ g}^{-1}$ in previous research [3]. The measurement of porosity depends on the surface area and pore volume. The observed difference can be attributed to the variation in gasification conditions between the two gasification models. In the PP20 model, MH is gasified at temperatures higher than $1000 \text{ }^\circ\text{C}$, using air as the reacting agent. The laboratory-scale gasification process of MH is conducted at lower temperatures compared to the PP20 system ($950 \text{ }^\circ\text{C}$), utilizing CO_2 and steam as the reacting agents [3]. Exposure to temperatures surpassing $1000 \text{ }^\circ\text{C}$ leads to a notable decrease in the porosity of char. The decrease in size can be ascribed to the disintegration of the pore structure and the liquefaction of inorganic mineral substances on the surface, resulting in the blockage of pores [17]. Furthermore, it has been confirmed that the utilization of CO_2 and steam as gasifying agents instead of air has a positive impact on the formation of

micro and meso-sized pores in the gasified char, thereby increasing the overall porosity of the char [18].

Table 1: Specific surface area and pore volume of MH gasified from PP20 system

S_{BET} ($\text{m}^2 \text{ g}^{-1}$)	S_{Micro} ($\text{m}^2 \text{ g}^{-1}$)	S_{Meso} ($\text{m}^2 \text{ g}^{-1}$)	V_{BET} ($\text{cm}^3 \text{ g}^{-1}$)	V_{Micro} ($\text{cm}^3 \text{ g}^{-1}$)	V_{Meso} ($\text{cm}^3 \text{ g}^{-1}$)
37.8	14	10.27	0.0375	0.0077	0.0138

Therefore, it is reasonable to suggest that the gasified char derived from MH on the PP20 system demonstrates a reduced adsorption capacity when compared to the gasified char generated at the laboratory levels. This assertion holds particular validity when the adsorption mechanism of the char primarily functions through physical mechanisms.

Elemental composition of char

The X-Ray Fluorescence study facilitated the determination of the inorganic composition of char, as depicted in Table 2. Furthermore, prior research has determined that the ash content of MH is around 3.10 wt% [3].

Table 2: Inorganic composition of MH gasified by the PP20 system

Inorganic content (%)					
K	Al	Ca	Fe	Other	Total
11.3	3.54	39.2	1.56	34.3	0.75

The ash component of the biomass feedstock consists of its inorganic elemental composition and remains constant during the thermochemical conversion process. Hence, the ash concentration in the feedstock serves as a measure of the overall quantity of inorganic components found in the char particles. Therefore, the organic and inorganic components of the char were computed and displayed in Table 3.

Table 3: Organic and inorganic composition of MH gasified by the PP20 system

Organic content (mg g^{-1})	Inorganic content (mg g^{-1})					
	K	Al	Ca	Fe	Other	Total
895	12	3.7	41.2	34.3	13.95	10.5

The analysis of the data indicates that the char sample, contains a significant amount of calcium (greater than 41 mg g^{-1}), iron (greater than 34 mg g^{-1}), and

potassium (approximately 12 mg g^{-1}) as part of its overall elemental composition. As a result, when comparing MH gasification at the laboratory scale to the MH char obtained from the PP20 system, it was observed that the MH char displayed a notably greater calcium content compared to potassium. This calcium content constituted a significant proportion of the inorganic content in the char sample [3]. The difference in gasification temperature between the pilot scale and the laboratory scale may have caused the potassium content in the char sample to decompose [19]. Furthermore, the analytical findings unveiled minute quantities of additional inorganic constituents, such as aluminum (Al), phosphorus (P), and sulfur (S). Significantly, it was observed that pilot-scale MH chars contained a small amount of Si, a recognized element that could potentially hinder the biomass gasification process [20–22].

The inhibitory function of inorganic constituents in char on gasification reactions has been verified to exert a more significant influence than morphological attributes. The emergence of active sites is commonly observed at the crystal edges of char, where there is a concentration of defects in the carbon crystal or catalytic mineral clusters. The impact of inorganic constituents on the kinetics of char gasification has been highlighted in prior research, with a specific focus on the catalytic properties of alkali and alkaline earth metals, namely K, Na, Ca, and Mg [23]. Among the elements present in lignocellulosic biomass composition, Na is relatively rare, while Mg has been found to have a negligible effect on the reactivity of biomass gasification processes.

The zeroth-order trend in the ratio of $K/(Si+P)$ in the MH char gasified at the pilot scale is observed, similar to the gasification process conducted at the laboratory scale [3]. This observation showcases the stability of the conversion rate, thereby guaranteeing uniformity in both the yield of synthesis gas and the conversion of char.

Moreover, the identification of alkali and alkaline earth metal elements, specifically K and Ca, on the surface of the char resulting from MH gasification, is associated with the augmentation of the material's alkalinity, consequently enhancing its capacity to adsorb CO_2 , a compound characterized by acidic properties [12,24]. The aforementioned attribute has the potential to facilitate the chemical adsorption mechanism of carbon dioxide gas by the char, as it encourages the creation of carbonate, bicarbonate, mineral, and various other compounds. Hence, the existence of K and Ca constituents in the char produced through MH

gasification indicates that this substance has the potential to be efficiently employed as a CO_2 adsorbent. Therefore, the analysis of the elemental composition of the char produced through MH gasification in the PP20 system can offer significant insights into the potential uses of this carbonaceous solid by-product.

CO₂ adsorbability

Fig 4 illustrates the results of CO_2 gas adsorption when using MH gasified char from the PP20 system. The results indicate that the material gained an additional mass of 3.54 wt% compared to the initial mass after a relatively long period (approximately 65 minutes). This mass gain corresponds to an adsorption capacity of 0.77 mmol CO_2 per gram of material. Furthermore, when transitioning to a stream of N_2 gas for sample regeneration, the material releases CO_2 much faster than the CO_2 adsorption time (about 10 minutes to completely release 100 % CO_2). This represents an advantage in CO_2 adsorption technology as it allows for the separation of CO_2 gas from the exhaust stream and its storage elsewhere. The measured CO_2 gas adsorption results are also consistent and compatible with the S_{BET} in Table 1. CO_2 gas molecules readily adsorb onto the surface of the biomass char due to its porous surface structure via physical mechanisms.

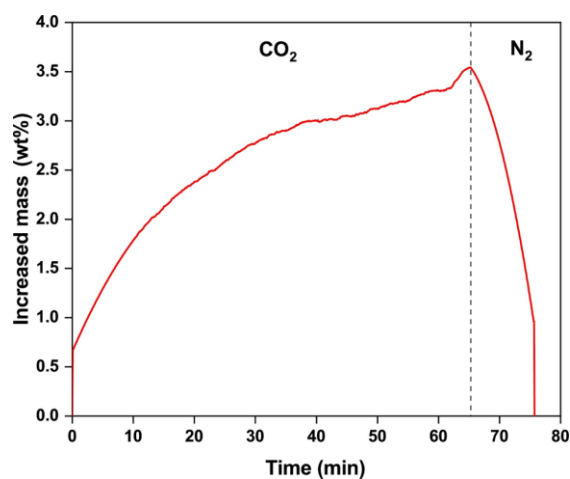


Fig. 4: CO_2 adsorption of MH gasified chars

Conclusion

The results obtained from the gasification of MH in a pilot scale system indicate that it is indeed feasible to use MH for energy generation and CO_2 adsorbent production in a commercial cascading manner. The MH chars exhibited a porous structure, with micropores being the most prominent. In addition, the

presence of numerous oxygen-containing and basic functional groups, along with a significant concentration of K and Ca on the surface, collectively resulted in a peak capacity for CO₂ adsorption of 0.77 mmol per gram of char.

These findings are highly significant in determining the appropriateness of MH as a replacement biomass feedstock for wood in biomass gasification technology, allowing for the simultaneous production of energy and synthesis of adsorbent materials. Both the economic feasibility and environmental sustainability of this promising thermochemical biomass conversion technology are enhanced by their contributions.

Acknowledgments

This research was funded by the University of Science and Technology of Hanoi for the emerging research group “Sustainable Energy and Environmental Development” (SEED).

References

- International Nuts and Dried Fruits Council. Nuts and dried fruits statistical yearbook 2022/2023 [Internet]. International Nuts and Dried Fruits Council Foundation; 2023 [cited 2023 Jul 18].
- Bada SO, Falcon RMS, Falcon LM, Makhula MJ. *J South Afr Inst Min Metall.* 115(8) (2015) 741–6. <http://dx.doi.org/10.17159/2411-9717/2015/V115N8A10>
- Vu NL, Nguyen ND, Nguyen VD, Tran-Nguyen PL, Nguyen HV, Dinh TMT, Nguyen HN. *Biomass Bioenergy.* 171 (2023) 106735. <https://doi.org/10.1016/j.biombioe.2023.106735>
- Linh Vu N, Nguyen ND, Thanh Dinh TM, Nguyen HN. *Ind Crops Prod.,* 206 (2023) 117662. <https://doi.org/10.1016/j.indcrop.2023.117662>
- Li K, Hostikka S, Dai P, Li Y, Zhang H, Ji J. *Proc Combust Inst.* 36(2) (2017) 3185–3194. <https://doi.org/10.1016/j.proci.2016.07.001>
- You S, Ok YS, Tsang DCW, Kwon EE, Wang CH. Towards practical application of gasification: a critical review from syngas and biochar perspectives. *Crit Rev Environ Sci Technol.* 48(22–24) (2018) 1165–1213. <https://doi.org/10.1080/10643389.2018.1518860>
- Marescaux A, Thieu V, Garnier J. *Sci Total Environ.* 643 (2018) 247–259. <https://doi.org/10.1016/j.scitotenv.2018.06.151>
- Dutcher B, Fan M, Russell AG. *ACS Appl Mater Interfaces.* 7(4) (2015) 2137–2148. <https://doi.org/10.1021/am507465f>
- Vega F, Cano M, Camino S, Navarrete B, Camino JA. *Int J Greenh Gas Control.* 73 (2018) 95–103. <https://doi.org/10.1016/j.ijggc.2018.04.005>
- Madzaki H, KarimGhani WAWAB, NurZalikhRebitanim, AzilBahariAlias. *Procedia Eng.* 148 (2016) 718–725. <https://doi.org/10.1016/j.proeng.2016.06.591>
- Promraksa A, Rakmak N. *Heliyon.* 6(5) (2020) e04019. <https://doi.org/10.1016/j.heliyon.2020.e04019>
- Yuan JH, Xu RK, Zhang H. *Bioresour Technol.* 102(3) (2011) 3488–97. <https://doi.org/10.1016/j.biortech.2010.11.018>
- Xu R kou, Zhao A zhen, Yuan J hua, Jiang J. *J Soils Sediments.* 12(4) (2012) 494–502. <https://doi.org/10.1007/s11368-012-0483-3>
- Dias D, Lapa N, Bernardo M, Godinho D, Fonseca I, Miranda M, et al.. *Waste Manag.* 65 (2017) 186–194. <https://doi.org/10.1016/j.wasman.2017.04.011>
- Brewer CE, Schmidt-Rohr K, Satrio JA, Brown RC.. *Environ Prog Sustain Energy.* 28(3) (2009) 386–96. <https://doi.org/10.1002/ep.10378>
- Benedetti V, Patuzzi F, Baratieri M. *Appl Energy.* 227 (2018) 92–99. <https://doi.org/10.1016/j.apenergy.2017.08.076>
- Liu T, Fang Y, Wang Y.. *Fuel.* 87(4–5) (2008) 460–6. <https://doi.org/10.1016/j.fuel.2007.06.019>
- Guizani C, Jeguirim M, Gadiou R, Escudero Sanz FJ, Salvador S. *Energy.* 112 (2016) 133–145. <https://doi.org/10.1016/j.energy.2016.06.065>
- Deng L, Ye J, Jin X, Zhu T, Che D. *Energy Procedia.* 142 (2017) 401–406. <https://doi.org/10.1016/j.egypro.2017.12.063>
- Dupont C, Nocquet T, Da Costa JA, Verne-Tournon C. *Bioresour Technol.* 102(20) (2011) 9743–9748. <https://doi.org/10.1016/j.biortech.2011.07.016>
- Strandberg A, Holmgren P, Wagner DR, Molinder R, Wiinikka H, Umeki K, et al. *Energy Fuels.* 31(6) (2017) 6507–14. <https://doi.org/10.1021/acs.energyfuels.7b00688>
- McKee DW. *Fuel.* 62(2) (1983) 170–175. [https://doi.org/10.1016/0016-2361\(83\)90192-8](https://doi.org/10.1016/0016-2361(83)90192-8)
- Trubetskaya A. *Energies.* 15(9) (2022) 3137. <https://doi.org/10.3390/en15093137>
- Walton KS, Abney MB, Douglas LeVan M. *Microporous Mesoporous Mater.* 91(1–3) (2006) 78–84. <https://doi.org/10.1016/j.micromeso.2005.11.023>